IMPACT-CATALYZED FORMATION OF THE LUNAR COMPOSITIONAL ASYMMETRY. Matt J. Jones[1] (matthew_jones@brown.edu), Alexander J. Evans[1], Brandon C. Johnson[2,3], Matthew B. Weller[1], Jeffrey C. Andrews-Hanna[4], Sonia M. Tikoo[5], and James T. Keane[6], [1]Department of Earth, Environmental and Planetary Sciences, Brown University, Providence, RI 02906, [2]Department of Earth, Atmospheric, and Planetary Sciences, Purdue University, [3]Department of Physics and Astronomy, Purdue University, [4]Lunar and Planetary Laboratory, University of Arizona, [5]Department of Geophysics, Stanford University, [6]Jet Propulsion Laboratory, California Institute of Technology.

Introduction: South Pole–Aitken (SPA) is the largest and oldest recognized impact basin on the Moon [1]. Located on the farside hemisphere (Fig. 1), SPA is nearly antipodal to the nearside geochemical province referred to as the Procellarum KREEP Terrane (PKT) [2]. The PKT signifies an unexplained lunar surface compositional asymmetry of KREEP, a geochemical component named for its enrichment in incompatible elements including potassium (K), rare earth elements (REE), and phosphorous (P) [3, 4].

Here, we demonstrate that impact-induced mantle heating [5, 6] from the SPA basin-forming event would have greatly influenced lunar interior dynamics and generated a subsurface hemispheric compositional asymmetry closely aligned with the present location of the PKT. Such a subsurface asymmetry provides a possible origin of the Moon's surface geochemical asymmetry, in particular, the presence of the PKT and the majority of lunar maria on the nearside hemisphere [7].

Thermochemical Evolution Model: Using a modified version of the 3-D spherical thermochemical evolution code CitcomS [8–10], we simulated the lunar interior subsequent to a SPA impact-induced thermal pulse, with special attention to the spatiotemporal evolution of a KREEP-bearing layer underlying the crust (Fig. 2). At the start of simulations, we prescribe a SPA-induced global temperature increase according to a Hugoniot-release model of impact shock heating [5, 11]. We utilize the best-fit SPA impact velocity of 10 km/s and projectile radius of 85 km [12, 13]. The prescribed temperature increase was benchmarked against impact heating results from iSALE models of SPA basin formation [14].

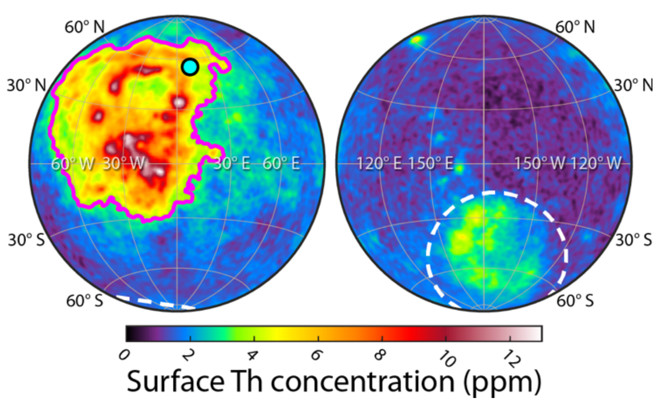

Figure 1: Lunar maps Th abundance maps [19] centered on the nearside (left) and farside (right) showcasing the lunar surface compositional asymmetry. PKT outlined in pink by 3.5 ppm Th contour [2]. SPA basin ellipse outlined in dashed white, basin-center antipode marked by cyan circle [20].

Initial Conditions. The silicate portion of the Moon is hypothesized to have fractionally crystallized from the lunar magma ocean (LMO) [3, 4]. During the late stages of LMO solidification, a global layer of low-viscosity, KREEP- and Th- bearing cumulates is expected to form immediately beneath the lunar crust [3, 4, 15]. Recent spectroscopic analyses suggest that these late-stage cumulates remained beneath the lunar farside crust at the time of the SPA impact [16], although it is uncertain whether the SPA basin was excavated prior to mixing of the underlying mantle. We thus examine two end member thermochemical scenarios for the state of the lunar mantle at the time of the SPA impact: the stratified case predicted to exist at the end of fractional LMO crystallization [15]; and a mixed case (with late-stage cumulates remaining immediately beneath the crust) with a mantle temperature ~1600 K, in line with constraints from SPA basin-formation simulations [12]. The stratified and mixed scenarios both evolve for 600 Myr, i.e., the approximate delay [1] between the SPA impact and the nearside Imbrium impact which is expected to have excavated subsurface KREEP in the PKT [17].

Results: As shown in Figure 2, the SPA-induced thermal anomaly generates a large upwelling plume centered beneath the SPA basin. The hemisphere-scale plume leads to lateral upper mantle flow, entraining and driving subcrustal KREEP-bearing late-stage cumulates toward the nearside hemisphere. Other plume structures (see Figure 2A) also result from the initially hot layer surrounding the core; the results thus are influenced by the structure of the initial thermal profile of the Moon.

In the stratified mantle scenario shown in Fig. 2A, hemispheric convection drives shallow lateral flow until at least 600 Myr after the SPA impact and generates a moderate asymmetry in shallow late-stage cumulates. The asymmetry in this scenario is characterized mostly by transport of farside late-stage cumulates toward the impact antipode. The late-stage cumulate layer thins significantly in the farside hemisphere and thickens minimally in the nearside hemisphere. The presence of late-stage cumulates in the nearside at 600 Myr after the SPA impact would allow for the Imbrium impact to excavate subsurface KREEP.

In the mixed mantle scenario shown in Fig. 2B, the initial upper mantle is warmer relative to the stratified case. The warmer upper mantle flows more readily, so transport of late-stage cumulates toward the impact antipode is enhanced globally. Late-stage cumulates are almost entirely removed from the farside and accumulate to more than double their original thickness across the nearside. Late-stage cumulate thickening is centered beneath the SPA antipode within the nearside PKT (Fig. 1), so this scenario generates a strong subsurface asymmetry that broadly aligns with the PKT. As with the stratified case, this scenario is consistent with excavation of KREEP by the Imbrium impact 400–600 Myr [1] after the SPA basin-forming event. Furthermore, the removal of late-stage cumulates from beneath much of the lunar crust is generally consistent with the lack of significant Th anomalies associated with basin ejecta across the farside hemisphere [17].

Implications: Our results indicate that hemispheric convection driven by the SPA-induced thermal anomaly is capable of transporting subcrustal late-stage cumulates to the nearside hemisphere early in lunar history. Constraints on the lunar upper mantle thermal structure at the time of the SPA impact [12] favor our mixed mantle temperature scenario, which results in a significant nearside-farside late-stage cumulate asymmetry. Our work suggests that the lunar surface geochemical asymmetry could be spatially related to a subsurface asymmetry in KREEP-bearing cumulates generated in the aftermath of the SPA basin-forming impact event.

Beyond the redistribution of KREEP, hemispheric convection driven by the SPA-induced thermal anomaly provides a mechanism by which a deeper lunar interior asymmetry could form. In simulations that consider more energetic SPA impacts (not shown here), a nearside downwelling antipodal to the SPA basin entrains dense late-stage cumulates and transports them deep into the nearside mantle. Such an asymmetrical mantle density distribution could affect characterizations of the interior of the Moon, e.g., derivations of crustal thickness [18] or explanations for the offset between the Moon's center of mass and center of figure.

The major reorganization of lunar interior dynamics caused by the SPA impact has not been widely factored into studies of lunar evolution, nor has its apparent influence on the formation of the lunar geochemical asymmetry. However, we demonstrate here that consideration of SPA-induced hemispheric convection is essential to the study of lunar evolution.

References: [1] Evans A. J. et al. (2018) *JGR: Planets, 123,* 1596-1617. [2] Jolliff B. L. et al. (2000) *JGR: Planets, 105*, 4197-4216. [3] Warren P. H. and Wasson J. T. (1979) *Rev. Geophys. Space Phys., 17,* 73-88. [4] Warren P. H. (1985) *Ann. Rev. Earth Planet. Sci., 13,* 201-240. [5] Watters W. A. (2009) *JGR, 114,* E02001. [6] Roberts, J. H. and Arkani-Hamed, J. (2012) *Icarus, 218,* 278-289. [7] Shearer C. K. et al. (2006) *Rev. Mineral. Geochem., 60*, 365–518. [8] Tan E. et al. (2006) *Geochem. Geophys. Geosys., 7,* No. 6. [9] Zhong S. et al. (2000) *JGR: Solid Earth, 105,* 11063-11082. [10] McNamara A. K. and Zhong S. (2004) *JGR: Solid Earth, 109,* B07402. [11] Pierazzo E. et al. (1997) *Icarus, 127,* 408-423. [12] Potter R. W. K. et al. (2012) *Icarus, 220*, 730–743. [13] Trowbridge A. J. et al. (2020) *Icarus, 352*, 113995. [14] Melosh H. J. et al. (2017) *Geology, 45*, 1063-1066. [15] Elkins-Tanton L. T. et al. (2011) *Earth Planet. Sci. Letters, 304,* 326-336. [16] Moriarty D. P. et al. (2021) *JGR: Planets, 126*, e2020JE006589. [17] Haskin L. A. (1998) *JGR: Planets, 103*, 1679–1689. [18] Wieczorek M. A. et al. (2013) *Science, 339,* 671-675. [19] Lawrence, D. J. et al. (2003) *JGR: Planets, 108,* 5102. [20] Garrick-Bethell, I. and Zuber, M. T. (2009) *Icarus, 204,* 399-40.

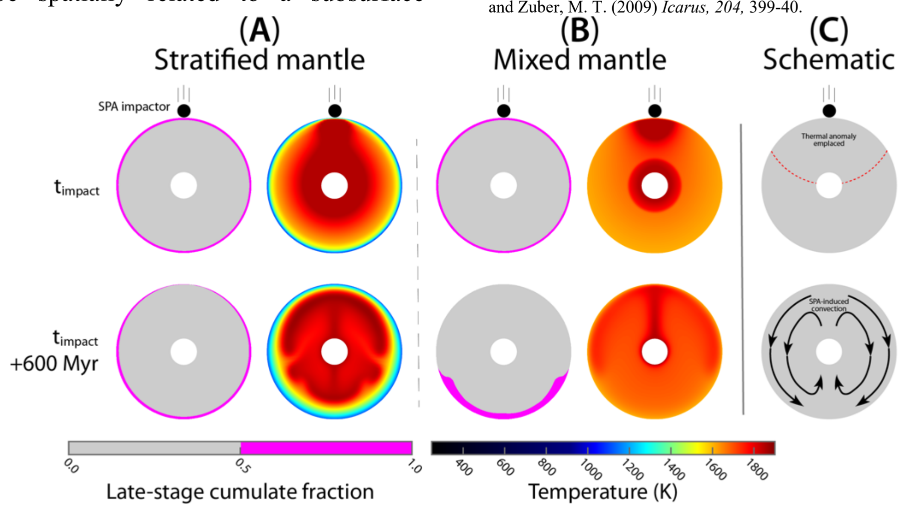

Figure 2: Cross-sections of lunar thermochemical evolution models at the time of the SPA impact (top) and 600 Myr after the SPA impact (bottom). Model scenarios with an initial lunar mantle that is (A) stratified and (B) mixed are shown. (A) and (B) show composition (left panels; late-stage cumulates in pink, the rest of the lunar mantle in grey) and temperature (right panels). (C) shows schematic cross sections that illustrate an arbitrary shock heating isotherm (top, dashed orange line) and the generalized pattern of hemisphere-scale convection catalyzed by the SPA impact (bottom, black arrows).